3602 *Biochemistry* **2010,** *49,* 3602–3610
DOI: 10.1021/bi9021999

BIOCHEMISTRY
including biophysical chemistry & molecular biology
Article

Critical Role of the Isoform-Specific Region in α1-Na,K-ATPase Trafficking and Protein Kinase C-Dependent Regulation[†]

Yoann Sottejeau,[‡] Aude Belliard,[‡] Marie-Josée Duran,[§,∥] Thomas A. Pressley,[§] and Sandrine V. Pierre*[,‡]

[‡]*Department of Physiology and Pharmacology, University of Toledo College of Medicine, Toledo, Ohio 43614, and* [§]*Center for Membrane Protein Research, Department of Cell Physiology and Molecular Biophysics, Texas Tech University Health Sciences Center, Lubbock, Texas 79430* [∥]*Current address: ELA Research Foundation, 26, rue de Londres, F-75009 Paris, France*

Received December 23, 2009; Revised Manuscript Received March 12, 2010

ABSTRACT: The isoform-specific region (ISR) is a region of structural heterogeneity among the four isoforms of the catalytic α-subunit of the Na,K-ATPase and an important structural determinant for isoform-specific functions. In the present study, we examined the role of a potential dileucine clathrin adaptor recognition motif [DE]XXXL[LI] embedded within the α1-ISR. To this end, a rat α1 construct where leucine 499 was replaced by a valine (as found in the α2 isoform sequence) was compared to wild-type rat α1 after stable expression in opossum kidney cells. Total Na,K-ATPase expression, activity, or *in situ* $^{86}Rb^{+}$ transport was not affected by the L499V mutation. However, surface Na,K-ATPase expression was nearly doubled. This increase was associated with a reduced rate of internalization from the cell surface of about 50% after a 4 h chase and became undetectable if clathrin-coated pit-mediated trafficking was blocked with chlorpromazine. Further, PKC-induced stimulation of Na,K-ATPase-mediated $^{86}Rb^{+}$ uptake was doubled in mutant-expressing cells, comparable to the chimera containing the intact α2-ISR. Similar results were observed when the potential motif was disrupted by means of an E495S mutation. These findings suggest that a dileucine motif embedded within the Na,K-ATPase α1-ISR plays a critical role in the surface expression of Na,K-ATPase α1 polypeptides at steady state and in the response to PKC activation.

The Na,K-ATPase is critical for maintaining the ionic gradients across the plasma membranes of animal cells. The primary contributor to overall catalysis, the α subunit, exists as four distinct isoforms (*1*). There are observed kinetic differences among these isoforms, but the subtlety of these distinctions makes them an unlikely basis for physiological significance, especially in humans (*2*, *3*). Instead, it has been suggested that the major functional distinction among the isoforms involves two issues: their regulation by intracellular effectors such as protein kinase C (PKC)[1] (*4*, *5*) and their localization in highly differentiated cells (*6*).

It could almost go without saying that the molecular basis underlying the differential response to regulation and targeting must reside within regions of structural divergence among the isoforms. Current research has focused on the role of two major regions of marked structural diversity: the amino-terminal domain and a 10-residue region near the center of the molecule, the isoform-specific region (ISR) (Figure 6A, K^{489}-L^{499} on the α1 polypeptide) (*7*, *8*). Earlier work with chimeras in which the central ISR of the rat α1- and α2-isoforms were exchanged suggests that this region plays a key role in the isoform-specific PKC regulation of pump activity (*9*). This prompted us to examine further the ISR sequence in α1 and α2. Alignment of the sequences revealed that the ISR of α1 contains a potential dileucine motif [DE]XXXL[LI] (*10*). Indeed, the pair of leucines is conserved among all of the known mammalian α1 sequences, although the presence of an equally conserved proline within the "polar" central portion of the region deviates somewhat from the consensus structure. Nevertheless, this motif could serve as a target for adaptor proteins that mediate membrane translocation, such as AP-2. The dileucines are disrupted in the ISR of α2 by substitution with a conserved valine, and we hypothesized that this motif in α1 could encourage translocation of pump complexes from the plasmalemma to intracellular vesicles, presumably via clathrin-coated vesicles and clathrin adaptor proteins (*11*, *12*). To test this hypothesis, two ISR mutants of the rat α1 sequence were characterized after heterologous expression in opossum kidney (OK) cells. The results presented here show that steady-state Na,K-ATPase cell surface expression was altered in both mutants, consistent with altered trafficking of the α1 protein from the cell membrane. Further, the observed PKC responses in these mutations were doubled relative to rat α1, further suggesting a role of the dileucine ISR in PKC-induced activation.

EXPERIMENTAL PROCEDURES

Expression Vectors, Site-Directed Mutagenesis, and Heterologous Expression. cDNAs encoding wild-type (WT) or modified ouabain-resistant rat α1 sequences were prepared as described (*9*) in the eukaryotic expression vector pRc/CMV

[†]This work has been supported by grants from the American Heart Association Texas Affiliate (98G-385), the National Center for Research Resources (RR-19799), and the National Heart, Lung, and Blood Institute, NIH (HL 36573).

*Corresponding author. Phone: 419-383-4182/4150. Fax: 419-383-2871. E-mail: Sandrine.Pierre@utoledo.edu.

[1]Abbreviations: CPZ, chlorpromazine; ISR, isoform-specific region; OK cells, opossum kidney cells; PMA, phorbol 12-myristate 13-acetate; PKC, protein kinase C; TCEP, tris(2-carboxyethyl)phosphine hydrochloride; YFP, yellow fluorescent protein.

 Published on Web 03/21/2010

(Invitrogen, San Diego, CA). All mutants were created by site-directed mutagenesis of WT or yellow fluorescent protein- (YFP-) tagged rat α1 constructs (QuickChange mutagenesis kit; Stratagene, La Jolla, CA), and the structures of the resulting mutant cDNAs were confirmed by direct sequencing of the altered regions. Stable heterologous expression was achieved by transfection of OK cells (CRL-1840; American Type Culture Collection) and subsequent selection of recipients with 3 μM ouabain, as we and others have described previously (*9*, *13*, *14*). This strategy takes advantage of the well-known reduced ouabain sensitivity of rodent Na,K-ATPase α1 polypeptide compared to other species. Indeed, a concentration of 3 μM ouabain is sufficient to kill nontransfected OK cells but not cells that express the introduced rat α1-derived forms. Expression of the expected exogenous sequences was confirmed by reverse transcription and polymerase chain reaction (PCR) as described (*9*, *15*).

Active Transport. Na,K-pump-mediated transport was assessed by measuring the ouabain-sensitive uptake of the K^+ congener, $^{86}Rb^+$, as previously described (*9*). Briefly, the difference in accumulation of radioisotope over 5 min at 37 °C was determined in cells exposed to standard culture medium with 3 μM or 1 mM ouabain. The effect of PKC activation was determined by treating confluent monolayers for 5 min with DMSO vehicle or the phorbol ester agonist, phorbol 12-myristate 13-acetate (PMA), prior to the addition of radiolabeled Rb^+. With the exception of one set of experiments (presented in Table 1 and explicitly labeled as such) the intracellular Na^+ concentration in the OK cells was increased with the ionophore monensin at a concentration of 20 μM.

Enzymatic Activity. The specific activity of Na,K-ATPase in whole cell lysates was determined from the hydrolysis of radiolabeled ATP as previously described (*16*). The difference in inorganic phosphate release from [γ-^{32}P]ATP (100 μCi/mmol) in the absence and presence of 3 mM ouabain was determined after a 30 min incubation at 37 °C in buffer containing 130 mM NaCl, 20 mM KCl, 3 mM $MgCl_2$, 3 mM ATP Na^+ salt, 25 mM histidine, 0.20 mM EGTA, and 3 mM NaN_3 (pH 7.5 at 25 °C). Hydrolysis rates were standardized against the amount of protein.

Fluorescence Imaging. Cells were grown on glass coverslips for 24 h followed by a 24 h period of exposure to cycloheximide (5 nM) prior to visualization using an inverted confocal argon and helium/neon laser scanning microscope (DM IRE2; Leica) equipped with a 63×/1.3 oil objective.

Biotinylation and Western Blotting. Total and surface protein abundances of the introduced α1 constructs were determined by electrophoresis and immunoblotting as described previously (*8*). Rat-derived α1 was detected with anti-NASE, a site-directed rabbit polyclonal antibody directed against the α1-ISR. Although some preparations of this antibody cross-react with the endogenous opossum subunit, we selected a preparation in which this cross-reactivity was minimal. In some experiments, immunoblotting results were confirmed by the use of 6F, a monoclonal antibody directed against chicken α subunit (*7*). Equal loading of the samples among the lanes of the gel was confirmed by probing with a commercial antibody against actin (Santa Cruz Biotechnology, Santa Cruz, CA).

The amount of introduced α1 expressed at the cell surface was detected by biotinylation following the recommended procedures of Gottardi et al. (*17*). Seventy percent confluent cells grown on 100 mm culture dishes were placed on ice, rinsed twice with ice-cold saline, and exposed twice to 1.5 mg/mL *N*-hydroxysulfosuccinimidobiotin in biotinylation buffer (10 mM triethanolamine, 2 mM $CaCl_2$, 150 mM NaCl, 250 mM sucrose, pH 9.0) for 25 min at 4 °C. Unreacted biotin was scavenged by a 20 min exposure to 100 mM glycine buffer at 4 °C, followed by two additional washes with saline. Cells were then solubilized in lysis buffer (1% Triton X-100, 150 mM NaCl, 5 mM EDTA, 50 mM Tris, pH 7.5) for 60 min on ice, and the resulting lysates were cleared by centrifugation at 14,000*g* for 10 min at 4 °C. Lysates were incubated overnight at 4 °C with streptavidin−agarose beads (Pierce) with end-over-end rotation. The beads were then washed twice with lysis buffer, twice with high-salt buffer (0.1% Triton X-100, 500 mM NaCl, 5 mM EDTA, 50 mM Tris, pH 7.5), and twice with no-salt wash buffer (10 mM Tris, pH 7.5). Bound proteins were eluted with sodium dodecyl sulfate-containing sample buffer for analysis by electrophoresis and immunoblotting as described above. To test whether any changes in surface expression of the introduced mutants were related to clathrin-mediated membrane recycling of the Na,K-ATPase, we studied the effect of chlorpromazine (CPZ) (Vetranal; Sigma), a cationic amphiphilic drug that inhibits clathrin-mediated membrane recycling by encouraging the removal of coated pits from the cell surface (*18*). Based on previous studies (*19*, *20*), we opted for a treatment that consisted of a 24-h pretreatment with 5 nM cycloheximide before exposure to 10 μM CPZ for 30 min followed by 4 h incubation in culture media. Evaluation of endocytosis of Na,K-ATPase was accomplished with a pulse−chase strategy. Cells were serum-starved and treated with 5 nM cycloheximide 24 h prior to the beginning of the experiment. First, proteins expressed at the cell surface were biotinylated as described above, quenched with PBS−glycine buffer, and brought back to normal culture conditions for 0 or 4 h. The remaining surface-bound biotin was then cleaved by treatment with tris(2-carboxyethyl)phosphine hydrochloride (TCEP) reducing agent (100 mM into 50 mM Tris, pH 7.4) for 30 min at 4 °C as described previously (*21*).

Na,K-ATPase Structure. The high-resolution structure of the pig Na,K-ATPase published by Morth et al. (*22*) was obtained using the Cn3D software from NCBI's Entrez retrieval service. The localization of the ISR on the pig structure was determined following alignment of the rat (NM012504) and pig (PDB ID 3138E) α1 isoform amino acid sequences obtained from the NCBI database. For the studies illustrated in Figure 6C,D, a probable structure was generated using the SWISS-MODEL best fit tool and refined using the built-in energy minimization tool. Gaps and breaks introduced into the sequences were repaired manually, and the structure was again refined using the energy minimization tool. The resulting structural models were visualized using PyMOL. Protein surfaces were also generated using the PyMOL software.

RESULTS

Characterization of α1-L499V. Our initial experiments focused on an α1 construct in which the first leucine of the putative dileucine motif (^{495}EPKHLLV^{501}) was replaced with a valine, as present in the sequence of α2 (^{492}PQSHVLV^{498}) (Figure 6A). Transfection of the α1-L499V construct into OK cells and selection as detailed in Experimental Procedures produced ouabain-resistant colonies, indicating that the mutant was capable of producing functional Na,K-ATPase. Qualitatively, confocal fluorescence microscopy studies of YFP-tagged WT and the L499V mutant did not show intracellular sites of accumulation of fluorescence, suggesting that the mutation did

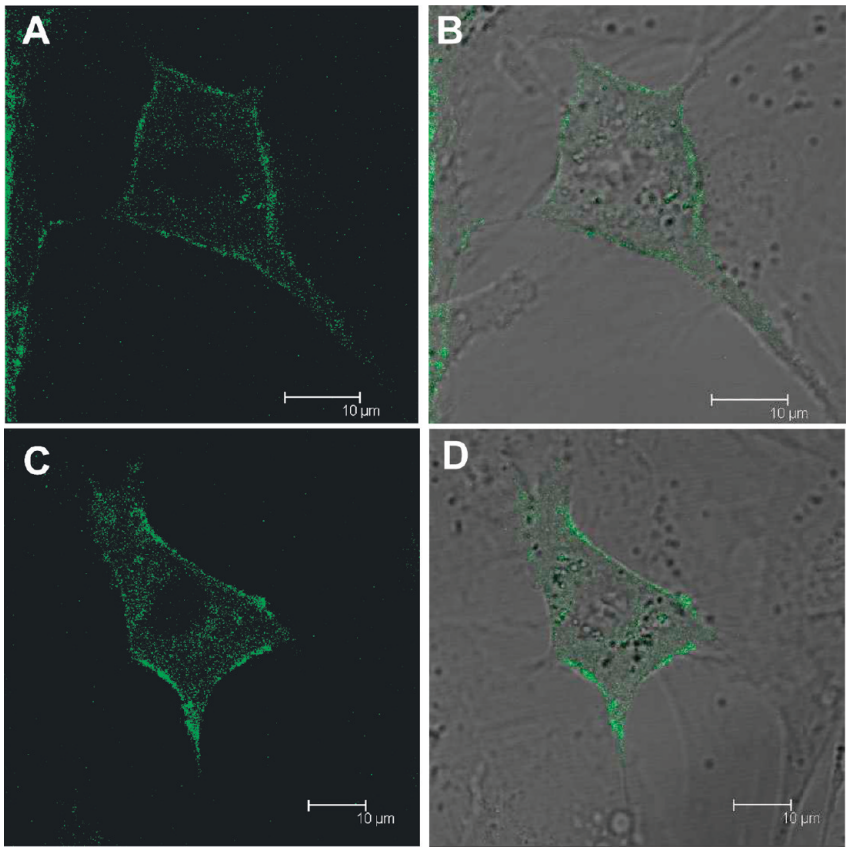

FIGURE 1: Fluorescence imaging of YFP-tagged WT (A, B) and L499V (C, D) rat Na,K-ATPase α1 transfected OK cells visualized by confocal microscopy as described in Experimental Procedures. (A, C) YFP fluorescence. (B, D) Merged picture of transmission microscopy and YFP fluorescence.

not result in a major change in the cellular processing and maturation of the α1 polypeptide (Figure 1). Consistent with this inference, introduction of the L499V mutation did not appear to affect quantitatively the total level of α1 subunit expression, as shown, from immunoblotting of cell lysates (Figure 2A). Moreover, *in situ* $^{86}Rb^{+}$ uptake (in the presence or absence of the Na^{+} ionophore monensin) and ouabain-sensitive Na,K-ATPase activity in OK cells expressing the α1-L499V mutant were not significantly different from that in cells expressing the wild-type rat α1 (Table 1).

Cell Surface Expression of α1-L499V. To test whether disruption of the potential ISR dileucine motif in the mutant could affect steady-state surface expression of the αl polypeptide, we conducted a series of experiments using cell surface biotinylation as detailed in Experimental Procedures. As shown in Figure 2B, immunodetection of the introduced wild-type α1 or the L499V mutant suggested a roughly 75% elevation in surface abundance in the mutant transfected cells ($P < 0.05$ vs α1). These results suggest that although the mutation had no effect on overall Na,K-ATPase expression, it did favor the expression of enzyme complexes at the plasmalemma. Shifts between the surface and intracellular sites could be mediated by a clathrin-dependent mechanism. To determine if the effect of the disruption of the α1-ISR putative dileucine on basal Na,K-ATPase surface expression involved coated pits, we compared the effect of chlorpromazine (CPZ) treatment on surface expression of α1 and α1-L499V. As shown in Figure 3A, the surface expression levels of α1 and α1-L499V were undistinguishable 4 h post-CPZ treatment. In addition, we verified that total expression levels of α1 and α1-L499V were still comparable following the treatment as shown in Figure 3B. Taken together, these results suggest that the difference we observed in Figure 2B involved recycling of clathrin-coated pits. To test whether the disruption of the dileucine motif may have decreased basal internalization of the L499V mutant compared to wild-type α1, we compared the time course of Na,K-ATPase removal from the cell surface using a combination of cell surface biotinylation and TCEP protection assay. As shown in Figure 4, the amount of Na,K-ATPases internalized in 4 h was significantly decreased by 2.6-fold in the mutant when compared to wild type ($P < 0.05$).

PKC Regulation of $^{86}Rb^{+}$ Uptake in Cells Expressing α1-L499V. We next determined what effects the changes in the dileucine motif would have on the response to PKC activation. As shown in Figure 5, a significant increase of 16 ± 1% in ouabain-sensitive $^{86}Rb^{+}$ uptake was observed following 5 min of PMA treatment in α1 transfected cells ($P < 0.01$ vs untreated α1, paired *t*-test). After exchange of the original α1-ISR for the α2 sequence, the PMA-induced activation reached 26 ± 4% ($P < 0.001$ vs untreated α1α2α1, paired *t*-test) and was significantly higher than the increase observed for the full-length α1 ($P < 0.05$), in agreement with our previous report (*9*). In α1-L499V transfected cells, the response to PMA treatment reached 26 ± 2% ($P < 0.001$ vs untreated α1-L499V, paired *t*-test), indistinguishable from the response of OK cells expressing the α1α2α1 chimera. It therefore appears that replacing L499 by a V is sufficient to mimic the effect of exchanging the entire ISR sequence.

ISR and L499V Location on the Na,K-ATPase Structure. If the central ISR of the α subunit plays a role in AP/clathrin-mediated shuttling of the Na,K-ATPase complex

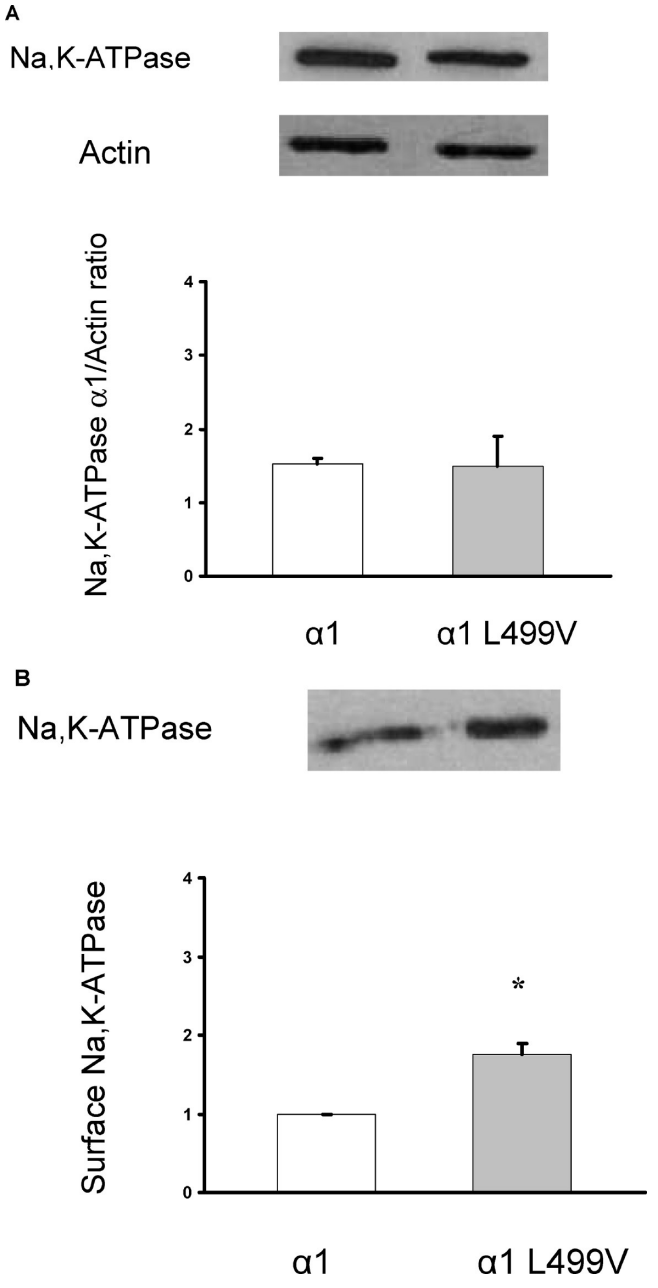

FIGURE 2: (A) Total abundance of rat α1 and α1-L499V in transfected OK cells. The upper panel depicts typical immunoblots of cell lysates probed with antibodies specific for α1 and actin. The lower panel depicts the pooled data relative to α1, represented as means ± SEM ($n = 4$). Values were compared using bilateral Student's t-test, and no significant difference was observed. (B) Surface expression of rat α1 and α1-L499V in transfected OK cells. The upper panel depicts a typical immunoblot of biotinylated membrane proteins recovered by affinity purification with streptavidin. The lower panel depicts the pooled data relative to α1, represented as means ± SEM ($n = 3$). Values were compared using bilateral Student's t-test. *, $P < 0.05$ vs α1.

between the plasmalemma and intracellular compartments, it must be accessible for interaction with other proteins. We examined the likely position of the ISR, taking advantage of the recent high-resolution structure obtained for the Na,K-ATPase complex from pig kidney (*22*). Homology modeling of the rat sequence against this structure suggests that the ISR of α protrudes into the cytoplasm from the N or "nucleotide-binding" domain, consistent with earlier models based on the sarcoplasmic reticulum Ca^{2+}-ATPase (*15*) (Figure 6B). At least

Table 1: Effect of α1-L499V Mutation on Rb^+ Transport and Ouabain-Sensitive ATPase Activity[a]

	OK α1	OK α1-L499V
Rb^+ transport without monensin	7.47 ± 0.38, $n = 11$	7.52 ± 1.11, $n = 14$
Rb^+ transport with monensin	9.25 ± 1.14, $n = 6$	9.15 ± 0.46, $n = 7$
ouabain-sensitive ATPase activity	0.42 ± 0.14, $n = 5$	0.52 ± 0.07, $n = 5$

[a]Na,K-ATPase-mediated transport was assayed in the absence or presence of 20 μM monensin. Uptakes are expressed as nmol of K^+ (mg of protein)$^{-1}$ min^{-1} and are quoted as means ± SEM with the indicated number of experiments. Ouabain-sensitive ATPase activities are expressed as μmol of P_i h^{-1} (mg of protein)$^{-1}$ and are quoted as means ± SEM with the indicated number of experiments. Values obtained for α1 and α1-L499V were compared using bilateral Student's t-test and were not found to differ significantly from one another.

theoretically, this places the ISR in an accessible position for interaction with intracellular partners such as clathrin APs.

Closer inspection of the likely surface of the molecule, however, suggested a more complex situation (Figure 6C). Leu-499 of rat α1 appears to be barely exposed to the solvent (panel A of Figure 6D). The homologous residue of rat α2 (Val-496) is similarly hidden. If anything, the position of Val-496 is within a pocket that may be even less accessible than the corresponding region of α1 (panel B of Figure 6D). The structural model for the L499V mutant suggests an intermediate condition. Although the pocket in which the valine is located appears more like that of α1, its accessibility may be compromised because the smaller side chain does not penetrate as readily to the surface, leaving a deeper hole than the wild-type subunit in the same region (panel C of Figure 6D). Taken together, the results from these structural analyses suggested that L499 is likely to be buried in the α1 structure (at least in the E2·P state of the pump cycle). It follows that the probable location of L499 does not suggest a direct role in protein−protein interaction such as those controlling membrane trafficking. Its position is not incompatible, however, with a key role for L499 as part of the overall dileucine motif [DE]XXXL[LI] in α1-ISR, which remains well exposed (loop in Figure 6B). To test further the role of the potential motif, we mutated the glutamate in position 495 (in green on Figure 6B) to a serine, altering the charge along the surface of this region.

Cell Surface Expression and PKC Response of α1-E495S. Transfection of the α1-E495S construct into OK cells produced ouabain-resistant colonies, indicating that the mutant was functional. The E495S mutation did not affect the total level of α1-subunit, as shown by immunodetection in cell lysates (Figure 7A). However, cell surface expression of α1-E495S was more than twice that observed for the wild-type α1 ($P < 0.05$), comparable to the increase observed for the α1-L499V mutant (Figure 7B). Finally, as shown in Figure 7C, Na,K-ATPase-mediated $^{86}Rb^+$ uptake increased by 29 ± 3% in response to PMA in α1-E495S transfected cells. Again, this increase was significantly higher than the increase observed for wild-type α1 ($P < 0.05$) and indistinguishable from the response observed for α1-L499V or the chimera α1α2α1.

DISCUSSION

The present study provides new supportive evidence for a regulatory role of one of the two major regions of marked structural diversity among the four isoforms of the Na,K-ATPase

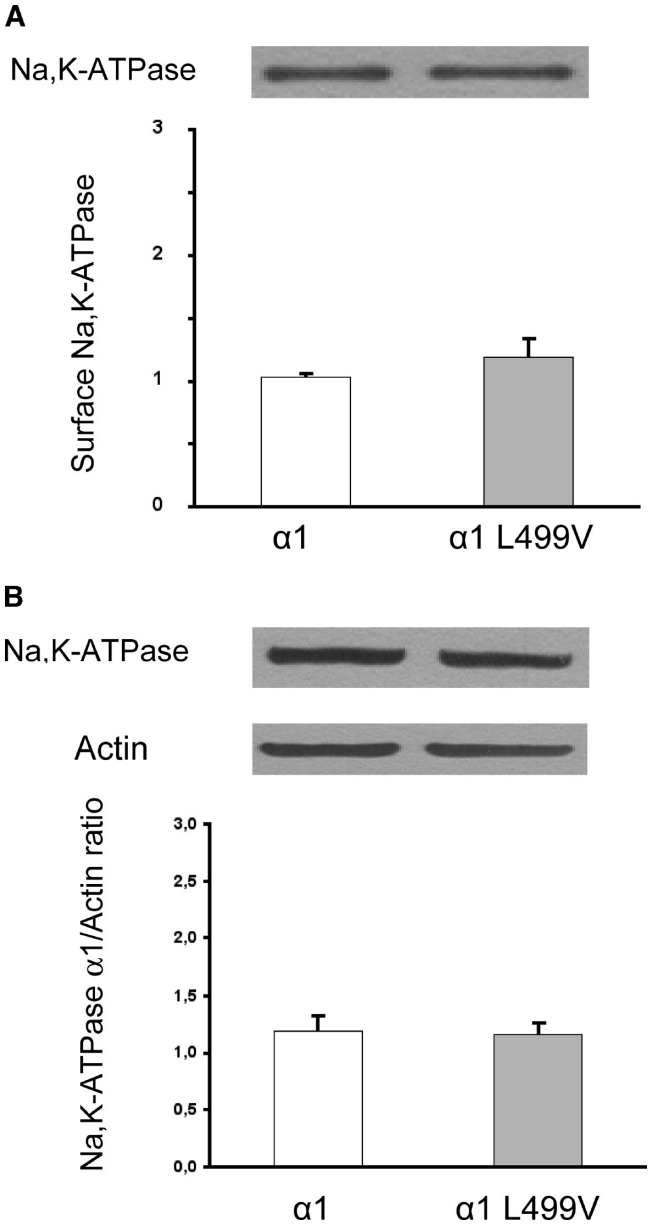

FIGURE 3: Effect of chlorpromazine treatment on surface (A) and total (B) expression of rat α1 and α1-L499V in transfected OK cells. Cells were treated with 10 μM chlorpromazine for 30 min, and surface or total protein lysates were prepared after 4 h of incubation at 37 °C. (A) The upper panel depicts a representative immunoblot of biotinylated surface membrane proteins recovered by affinity purification with streptavidin. The lower panel depicts the pooled data relative to α1, represented as means ± SEM (n = 7). (B) The upper panel shows representative immunoblots of cell lysates probed with antibodies specific for α1 and actin. The lower panel depicts the pooled data relative to α1, represented as means ± SEM (n = 7). Values were compared using bilateral Student's t-test, and no significant difference was observed.

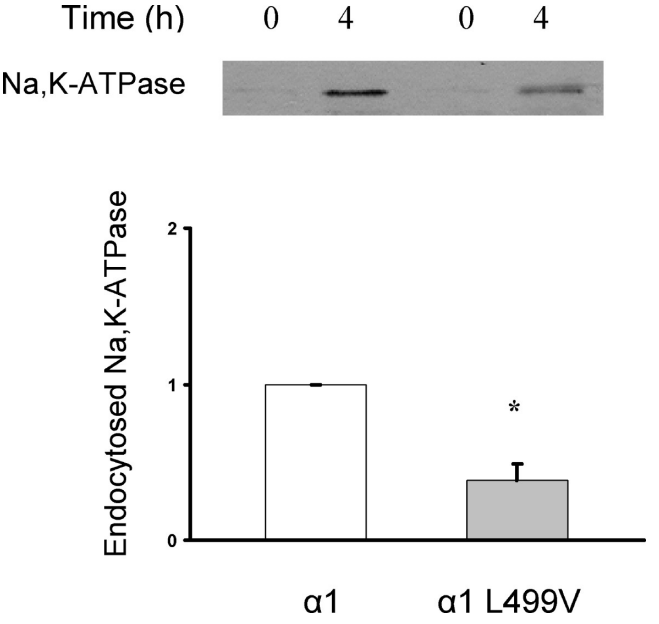

FIGURE 4: Na,K-ATPase endocytosis of wild-type α1 and L499V in transfected OK cells. The upper panel depicts a typical immunoblot of biotinylated endocytosed membrane proteins after 0 and 4 h at 37 °C recovered by affinity purification with streptavidin. The lower panel depicts the pooled data relative to wild-type α1, represented as means ± SEM (n = 3). Values were compared using bilateral Student's t-test. *, $P < 0.05$ vs the corresponding wild-type α1.

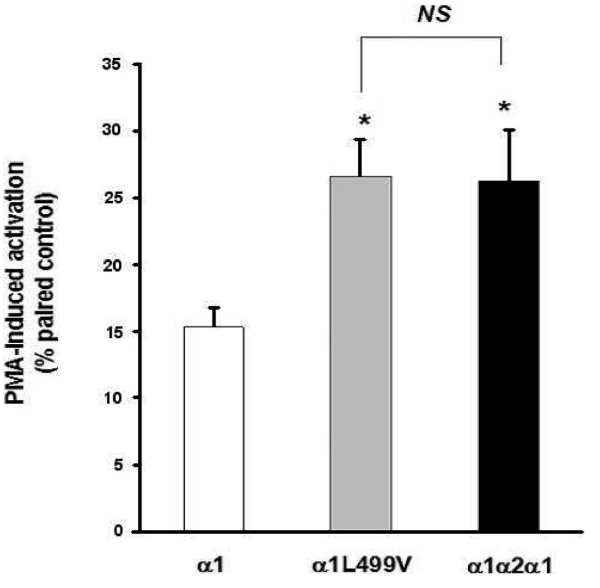

FIGURE 5: Effect of L499V mutation on PMA-dependent activation of α1 Na,K-ATPase-mediated Rb^+ transport. Na,K-ATPase-mediated transport was assayed in attached cells by measuring the ouabain-sensitive uptake of the K^+ congener, $^{86}Rb^+$. PKC activation was induced by a 5 min exposure of the cells to 10 μM PMA prior to the addition of Rb^+ and compared to paired control plates of cells exposed for 5 min to the same amount of vehicle alone (DMSO). Values are means ± SEM (n = 8−11) of uptake induced by PMA exposure, expressed in percent of their paired controls (same transfection group, same passage, same day). Values were compared using one-way ANOVA followed by Tukey's multiple comparison tests. NS, nonsignificant. *, $P < 0.05$ vs wild-type α1.

catalytic subunit: the isoform-specific region (ISR) (Figure 6A, K^{489}-L^{499} on the α1 polypeptide). On the basis of the functional characterization of two mutants where the potential dileucine recognition motif [DE]XXX[LI] in α1-ISR was disrupted, we propose that the ISR is involved in (1) trafficking of the α1 protein from the cell membrane under basal conditions and (2) the change in ion-pumping rate in response to PKC stimulation.

Effect of the Mutations at Steady State. The biotinylation experiments revealed an increased abundance of about 80% for both mutants in the plasma membrane, relative to the wild-type rat α1 subunit (Figures 2B and 7B). Despite this increase, we could not detect differences in total exogenous subunit nor Na,K-ATPase specific activity in cell lysates. It follows that the proportion of α1 subunit allocated to the surface must have been

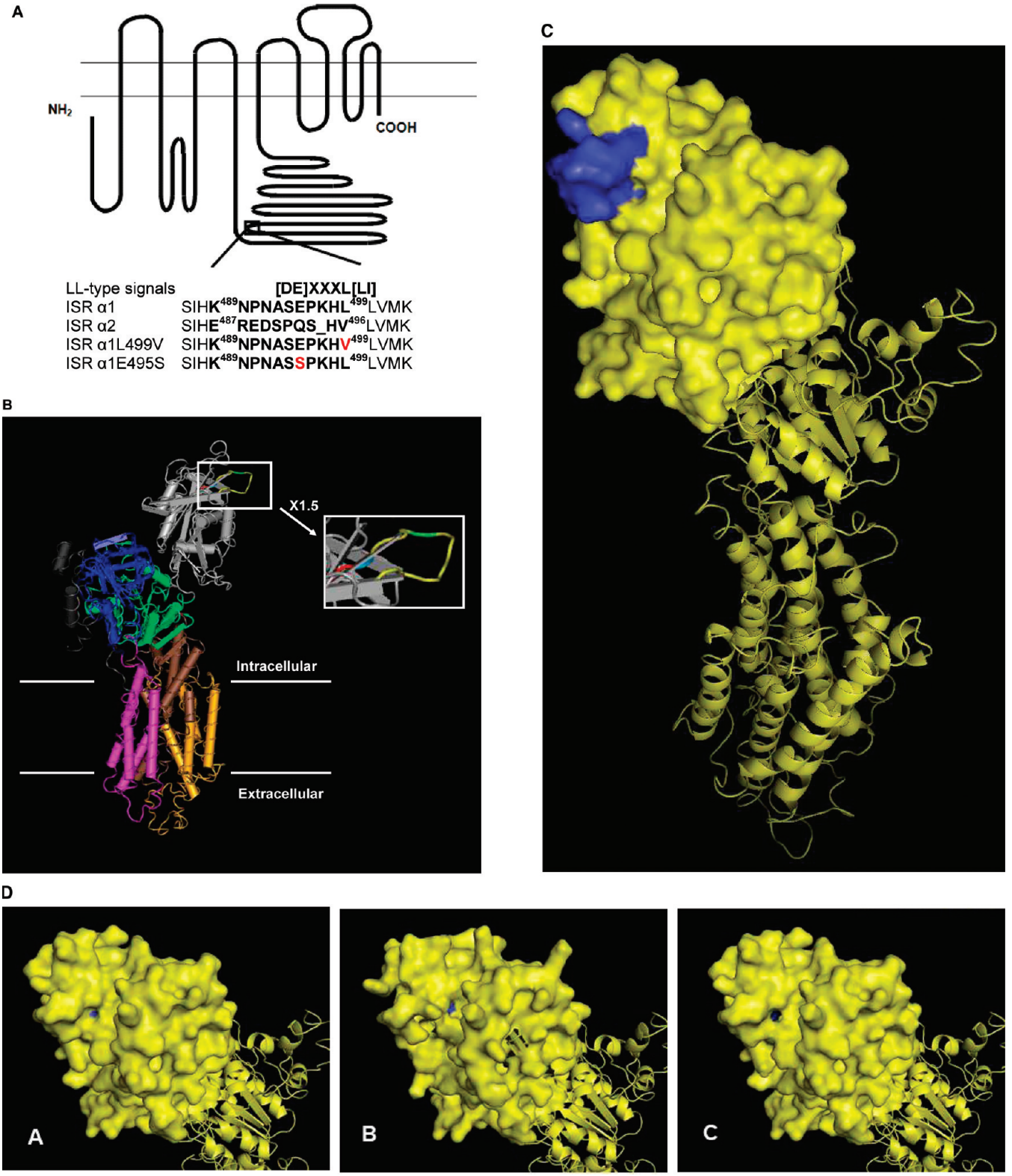

FIGURE 6: (A) Position and sequence comparison of the central isoform-specific regions (ISR) in the wild-type α1 and α2 catalytic subunits of the Na,K-ATPase from rat. The open box represents the location of the ISR. Mutated residues in the constructs used in the present study are shown in red. The sequence numbers of the boundary amino acids of the α1- and α2-ISR are indicated. (B) Likely position of the central ISR in the structure of the α1 subunit from the high-resolution structure of pig Na,K-ATPase (*22*) as deduced from homology modeling against the α1 subunit from rat. In the structure, the P-domain is depicted in green, the A-domain in blue, and the N-domain in gray. In the gray domain, the residues forming the ISR are depicted in yellow, E495 is in green, L499 is in blue, and L500 is in red. (C) Putative location of the dileucine motif in the structure of the α1, α2, and α1-L499V variant of the subunits from rat. (D) Leu-499 is identified by blue in the model for α1 (panel A). Val-496 is identified by blue in the model for α2 (panel B). The substitutent Val-499 is identified by blue in the model for α1-L499V (panel C).

larger in cells expressing the L499V mutant, and total exogenous expression was comparable for both wild-type and mutant forms.

It is probably not surprising that a mutation that alters trafficking in response to kinase activation would also influence basal

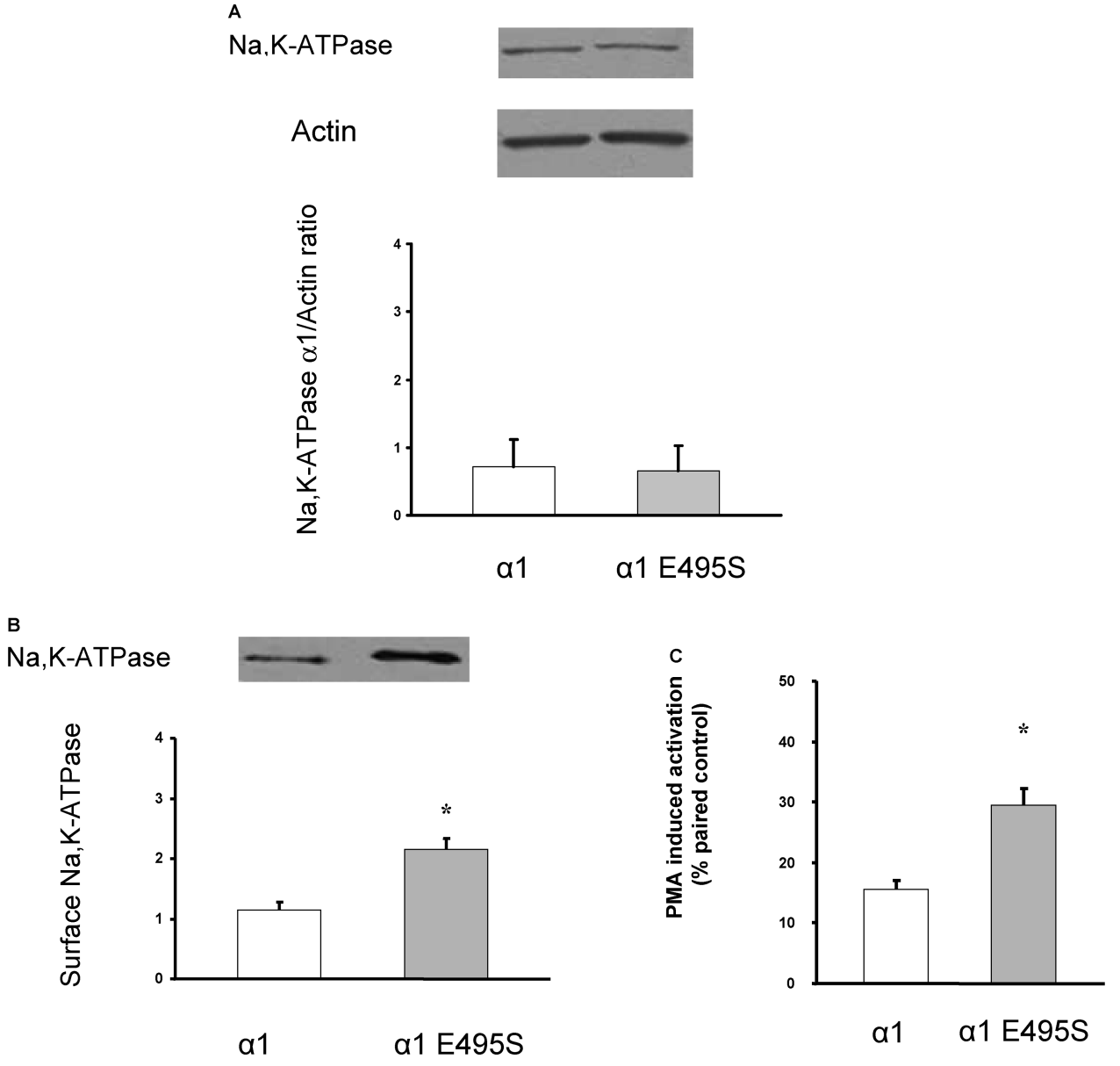

FIGURE 7: Effect of the E495S mutation on surface expression and PMA-dependent activation of α1 Na,K-ATPase-mediated Rb^+ transport. (A) Total abundance of rat α1 and α1-E495S in transfected OK cells. The upper panel depicts typical immunoblots of cell lysates probed with antibodies specific for α1 and actin. The lower panel depicts the pooled data relative to α1, represented as means ± SEM ($n = 3$). Values were compared using bilateral Student's *t*-test, and no significant difference was observed. (B) Surface expression of rat α1 and α1-E495S in transfected OK cells. The upper panel depicts a typical immunoblot of biotinylated membrane proteins recovered by affinity purification with streptavidin. The lower panel depicts the pooled data relative to α1, represented as means ± SEM ($n = 3$). Values were compared using bilateral Student's *t*-test. *, $P < 0.05$ vs α1. (C) Na,K-ATPase-mediated transport was assayed in attached cells by measuring the ouabain-sensitive uptake of the K^+ congener, $^{86}Rb^+$. PKC activation was induced by a 5 min exposure of the cells to 10 μM PMA prior to the addition of Rb^+ and compared to paired control plates of cells exposed for 5 min to the same amount of vehicle alone (DMSO). Values are means ± SEM ($n = 5$) of uptake induced by PMA exposure, expressed in percent of their paired controls (same transfection group, same passage, same day). Values were compared using bilateral Student's *t*-test. *, $P < 0.05$ vs the corresponding wild-type α1.

distribution of the enzyme complex, and the data presented in Figure 4 indeed suggest that the L499V mutation decreased the rate of Na,K-ATPase removal from the cell surface. Furthermore, the difference in basal cell surface expression between α1 and the mutant was no longer observed after CPZ treatment (Figure 3A), suggesting that the underlying mechanism involved the clathrin-coated pit recycling pathway. Additional unanticipated effects of the mutation may be evident when comparing the observed rates of transport and apparent surface abundance. Despite the elevated surface expression seen in α1-L499V transfected cells, their Na,K-ATPase-mediated uptake of $^{86}Rb^+$ was indistinguishable from that of cells expressing endogenous wild-type subunit (Table 1). Such a discrepancy suggests that the steady-state catalytic turnover of the L499V-containing enzyme complexes may have been lower than those containing wild-type proteins. This could simply reflect a somewhat lower intracellular Na^+ concentration (or more rigorously, its thermodynamic activity) in the mutant-expressing cells. That this was not the case is demonstrated by the effects on transport elicited by monensin. Both wild-type- and L499V-expressing cells increased their Na,K-ATPase-mediated transport by about 23% in the presence of the ionophore, which presumably increased intracellular Na^+ to near saturating concentrations. The similarity in response to monensin implies that the pumps in both cell

types were operating at comparable points on the concentration−activity curves for intracellular Na^+. Moreover, the relatively modest increases in transport seen with the addition of monensin suggest that the concentration of Na^+ inside both cell types was mildly elevated relative to nontransfected cells. Many cells in culture will respond with an approximate doubling of Na,K-ATPase-mediated transport in the presence of monensin, reflecting an intracellular Na^+ concentration near the enzyme's $K_{1/2}$. Given that the transfected OK cells used in this study were maintained in a low dose of ouabain sufficient to inhibit endogenous enzyme, an elevation in intracellular Na^+ would therefore not be unexpected.

Effect of the Mutations on PKC-Induced Stimulation of $^{86}Rb^+$ Uptake. Both mutations produced an increase in pump-mediated transport when OK cells were exposed acutely to phorbol esters that was roughly twice that seen with the wild-type subunit (Figures 5 and 7C). This suggests that Leu-499 and Glu-495 of the α1-ISR contribute to the regulation of the Na,K-ATPase-mediated ion transport by PKC attributed to this region in earlier work (*9*).

Data accumulated by several laboratories indicate that PKC regulates the cycling of pumps to and from the plasma membrane. For instance, activation of PKC produces clear shifts in the distribution of the pump that are mediated (at least in part) by modulation of clathrin-dependent endocytosis (*23*−*25*). Further studies are warranted to determine whether the mutations characterized here indeed interfere with this process. In favor of a physiological role of isoform-specific mechanisms in agonist-mediated regulation, Teixeira et al. (*26*) found that treatment of neostriatal neurons with dopamine decreases the amount of α2 in the membrane, without altering α1 abundance. Work by others argues that the second leucine of the dileucine motif is less critical. Doné et al. (*27*), for example, found that mutations in Leu-500 in rat α1 were not sufficient to alter PMA-induced activation. Similarly, studies with other proteins have suggested that the second leucine is less important in adaptor protein binding (*28*). Of course, the current work cannot exclude the contributions of other regions of the α subunit to membrane translocation nor does it identify the proteins responsible for targeting α.

Some proteins that are sorted via dileucine-based motifs are regulated by direct phosphorylation of a serine within the motif (*29*). Indeed, the ISR of rat contains a serine (Ser-494) in the same position as a serine within the dileucine motif of the T cell receptor that is targeted by PKC (*30*). This mechanism seems unlikely as an explanation for the Na,K-ATPase because the serine residues of α1 targeted by PKC are located in the amino terminus. Although this region was not resolved in the structure proposed by Morth et al. (*22*), its likely position within the high-resolution model is well away from the ISR, minimizing the likelihood of direct interactions between the two regions.

Taken together, these data suggest that a dileucine motif of the type [DE]XXXL[LI] in the Na,K-ATPase α1-ISR plays a role in surface expression of the polypeptide and in the enzyme response to PKC stimulation. Additional mutations and further structural modeling may shed some light on the precise underlying mechanism, and one can also expect that increased efforts will be directed toward direct identification of the various adaptor proteins responsible for the sorting of this important enzyme complex.

ACKNOWLEDGMENT

The authors appreciate the assistance of Deborah Carr, Ryan M. Downey, and Dr. Raymond E. Willis and are grateful to Dr. Ting Cai and Dr. Zi-Jian Xie for suggestions and discussions.

REFERENCES

1. Blanco, G., and Mercer, R. W. (1998) Isozymes of the Na-K-ATPase: heterogeneity in structure, diversity in function. *Am. J. Physiol. 275*, F633–650.
2. Crambert, G., Hasler, U., Beggah, A. T., Yu, C., Modyanov, N. N., Horisberger, J. D., Lelievre, L., and Geering, K. (2000) Transport and pharmacological properties of nine different human Na, K-ATPase isozymes. *J. Biol. Chem. 275*, 1976–1986.
3. Wang, J., Velotta, J. B., McDonough, A. A., and Farley, R. A. (2001) All human Na(+)-K(+)-ATPase alpha-subunit isoforms have a similar affinity for cardiac glycosides. *Am. J. Physiol. Cell Physiol. 281*, C1336–1343.
4. Blanco, G., Sanchez, G., and Mercer, R. W. (1998) Differential regulation of Na,K-ATPase isozymes by protein kinases and arachidonic acid. *Arch. Biochem. Biophys. 359*, 139–150.
5. Nishi, A., Fisone, G., Snyder, G. L., Dulubova, I., Aperia, A., Nairn, A. C., and Greengard, P. (1999) Regulation of Na^+, K^+-ATPase isoforms in rat neostriatum by dopamine and protein kinase C. *J. Neurochem. 73*, 1492–1501.
6. Song, H., Lee, M. Y., Kinsey, S. P., Weber, D. J., and Blaustein, M. P. (2006) An N-terminal sequence targets and tethers Na^+ pump alpha2 subunits to specialized plasma membrane microdomains. *J. Biol. Chem. 281*, 12929–12940.
7. Takeyasu, K., Lemas, V., and Fambrough, D. M. (1990) Stability of Na(+)-K(+)-ATPase alpha-subunit isoforms in evolution. *Am. J. Physiol. 259*, C619–630.
8. Pressley, T. A. (1992) Phylogenetic conservation of isoform-specific regions within alpha-subunit of Na(+)-K(+)-ATPase. *Am. J. Physiol. 262*, C743–751.
9. Pierre, S. V., Duran, M. J., Carr, D. L., and Pressley, T. A. (2002) Structure/function analysis of Na(+)-K(+)-ATPase central isoform-specific region: involvement in PKC regulation. *Am. J. Physiol. Renal Physiol. 283*, F1066–1074.
10. Kirchhausen, T. (1999) Adaptors for clathrin-mediated traffic. *Annu. Rev. Cell Dev. Biol. 15*, 705–732.
11. Simmen, T., Honing, S., Icking, A., Tikkanen, R., and Hunziker, W. (2002) AP-4 binds basolateral signals and participates in basolateral sorting in epithelial MDCK cells. *Nat. Cell Biol. 4*, 154–159.
12. Brodsky, F. M., Chen, C. Y., Knuehl, C., Towler, M. C., and Wakeham, D. E. (2001) Biological basket weaving: formation and function of clathrin-coated vesicles. *Annu. Rev. Cell Dev. Biol. 17*, 517–568.
13. Jewell, E. A., and Lingrel, J. B. (1991) Comparison of the substrate dependence properties of the rat Na,K-ATPase alpha 1, alpha 2, and alpha 3 isoforms expressed in HeLa cells. *J. Biol. Chem. 266*, 16925–16930.
14. Vilsen, B. (1997) Leucine 332 at the boundary between the fourth transmembrane segment and the cytoplasmic domain of Na^+,K^+-ATPase plays a pivotal role in the ion translocating conformational changes. *Biochemistry 36*, 13312–13324.
15. Duran, M. J., Pierre, S. V., Carr, D. L., and Pressley, T. A. (2004) The isoform-specific region of the Na,K-ATPase catalytic subunit: role in enzyme kinetics and regulation by protein kinase C. *Biochemistry 43*, 16174–16183.
16. Pressley, T. A., Haber, R. S., Loeb, J. N., Edelman, I. S., and Ismail-Beigi, F. (1986) Stimulation of Na,K-activated adenosine triphosphatase and active transport by low external K^+ in a rat liver cell line. *J. Gen. Physiol. 87*, 591–606.
17. Gottardi, C. J., Dunbar, L. A., and Caplan, M. J. (1995) Biotinylation and assessment of membrane polarity: caveats and methodological concerns. *Am. J. Physiol. 268*, F285–295.
18. Wang, L. H., Rothberg, K. G., and Anderson, R. G. (1993) Mis-assembly of clathrin lattices on endosomes reveals a regulatory switch for coated pit formation. *J. Cell Biol. 123*, 1107–1117.
19. Guevara, E. A., de Lourdes Barriviera, M., Hasson-Voloch, A., and Louro, S. R. (2007) Chlorpromazine binding to Na^+, K^+-ATPase and photolabeling: involvement of the ouabain site monitored by fluorescence. *Photochem. Photobiol. 83*, 914–919.
20. Liu, J., Kesiry, R., Periyasamy, S. M., Malhotra, D., Xie, Z., and Shapiro, J. I. (2004) Ouabain induces endocytosis of plasmalemmal Na/K-ATPase in LLC-PK1 cells by a clathrin-dependent mechanism. *Kidney Int. 66*, 227–241.

21. Klisic, J., Zhang, J., Nief, V., Reyes, L., Moe, O. W., and Ambuhl, P. M. (2003) Albumin regulates the Na^+/H^+ exchanger 3 in OKP cells. *J. Am. Soc. Nephrol. 14*, 3008–3016.
22. Morth, J. P., Pedersen, B. P., Toustrup-Jensen, M. S., Sorensen, T. L., Petersen, J., Andersen, J. P., Vilsen, B., and Nissen, P. (2007) Crystal structure of the sodium-potassium pump. *Nature 450*, 1043–1049.
23. Efendiev, R., Bertorello, A. M., Pressley, T. A., Rousselot, M., Feraille, E., and Pedemonte, C. H. (2000) Simultaneous phosphorylation of Ser11 and Ser18 in the alpha-subunit promotes the recruitment of Na(+),K(+)-ATPase molecules to the plasma membrane. *Biochemistry 39*, 9884–9892.
24. Bertorello, A. M., Komarova, Y., Smith, K., Leibiger, I. B., Efendiev, R., Pedemonte, C. H., Borisy, G., and Sznajder, J. I. (2003) Analysis of Na^+,K^+-ATPase motion and incorporation into the plasma membrane in response to G protein-coupled receptor signals in living cells. *Mol. Biol. Cell 14*, 1149–1157.
25. Khundmiri, S. J., Bertorello, A. M., Delamere, N. A., and Lederer, E. D. (2004) Clathrin-mediated endocytosis of Na^+,K^+-ATPase in response to parathyroid hormone requires ERK-dependent phosphorylation of Ser-11 within the alpha1-subunit. *J. Biol. Chem. 279*, 17418–17427.
26. Teixeira, V. L., Katz, A. I., Pedemonte, C. H., and Bertorello, A. M. (2003) Isoform-specific regulation of Na^+,K^+-ATPase endocytosis and recruitment to the plasma membrane. *Ann. N.Y. Acad. Sci. 986*, 587–594.
27. Done, S. C., Leibiger, I. B., Efendiev, R., Katz, A. I., Leibiger, B., Berggren, P. O., Pedemonte, C. H., and Bertorello, A. M. (2002) Tyrosine 537 within the Na^+,K^+-ATPase alpha-subunit is essential for AP-2 binding and clathrin-dependent endocytosis. *J. Biol. Chem. 277*, 17108–17111.
28. Dietrich, J., Kastrup, J., Nielsen, B. L., Odum, N., and Geisler, C. (1997) Regulation and function of the CD3gamma DxxxLL motif: a binding site for adaptor protein-1 and adaptor protein-2 in vitro. *J. Cell Biol. 138*, 271–281.
29. Geisler, C., Dietrich, J., Nielsen, B. L., Kastrup, J., Lauritsen, J. P., Odum, N., and Christensen, M. D. (1998) Leucine-based receptor sorting motifs are dependent on the spacing relative to the plasma membrane. *J. Biol. Chem. 273*, 21316–21323.
30. Dietrich, J., Hou, X., Wegener, A. M., Pedersen, L. O., Odum, N., and Geisler, C. (1996) Molecular characterization of the di-leucine-based internalization motif of the T cell receptor. *J. Biol. Chem. 271*, 11441–11448.